УДК 551.463.5

© *T. M. Radomyslskaya, I. M. Levin*
Saint-Petersburg Department of the P. P. Shirshov Institute of Oceanology of RAS, Russia
ocopt@yandex.ru

POSSIBILITY OF OIL POLLUTION DETECTION ON ICE COVER OF SEA SURFACE

On the basis of review of ice, snow and oil optical properties the analysis of the possibility of detecting oil pollution on the lower ice/water boundary is presented. The cases of observation from above by standard TV-system at daylight and from below by underwater laser-pulsed imaging system and the moving narrow-angle receiver are considered. It was shown that if the rare case of the pure crystal ice is excluded, observation from above under natural illumination is possible when the maximum ice thickness (without snow) is less than one meter. Observation from below by use of laser system is possible independently of snow presence and ice thickness from depth up to 30 m in the coastal waters and more than 40 m in ocean waters. If the moving narrow-angle receiver with an axis directed to zenith is used at daylight, the contrast oil-ice equals almost unity.

Key words: oil pollutions, sea surface, ice, snow, seawater, underwater imaging.

Control of environmental conditions in the ice-infested seas of the Arctic region has essential specificity compared to water areas of the middle latitudes. The main problem is the ice cover that exists throughout most of the year as compact ice field. Ice cover makes it impossible to apply many traditional remote methods of environmental monitoring and creates considerable difficulties for applying contact methods.

Fig. 1 demonstrates the oil film on the sea surface photographed by authors from helicopter over the Black Sea in UV spectral range. One can see that the image contrast is rather high. However, in the presence of ice and snow the problem of observation of oil pollution becomes more complex.

The remote sensing methods used for detecting oil pollutions on the ice and snow cover are based on illumination of ice-water layer with an oil film on the lower ice surface by natural or artificial light and receiving reflected or transmitted light by optical system. For observation in daylight the pollution can be detected if the apparent oil-ice contrast (C) exceeds the threshold value C_{th}. Under artificial laser illumination the signal/noise ratio (Ψ) should exceed threshold value Ψ_{th}. The image parameters C and Ψ depend on parameters of the imaging system, geometrical and optical parameters of the ice, oil film and water. The latter are inherent optical properties (IOP), namely, the extinction (c), absorp-

Fig. 1. Photo of the oil film on the sea surface done from TV-system screen.
Flight altitude 150 m, viewing angle 40°,
oil spot square 47 575 m^2.

tion (a), scattering (b) and backscattering (b_b) coefficients. Note that water IOP and methods of computing the light field in water have been studied thoroughly (e. g., [1, 2], while known data on IOP of snow and ice are often contradictory and have not been adequately investigated. In the next section, a short review is provided of optical properties of the ice, snow and oil.

The optical properties of ice, snow and oil. The optical properties of ice and snow are determined by their age and structure, temperature, mutual position and orientation of ice crystals, ice salinity, existence of bubbles in its body, as well as by weather and season. The apparent optical properties of ice and snow given in the literature are mainly the vertical attenuation and absorption coefficients and the reflectance (albedo). The average vertical attenuation coefficient (k) for snow and ice of thickness z is determined by the equation $E_{\text{snow, ice}}(z) = E(0)\exp(-k_{\text{snow, ice}}\, z_{\text{snow, ice}})$, where $E(z)$ and $E(0)$ are downwelling irradiance on the lower and upper boundaries of snow or ice layers, z_{snow} and z_{ice} are snow and ice thicknesses.

Long-run measurements of under-ice and reflected radiation in the lake water [3] have showed that albedo of the snow-ice cover varied strongly seasonally and from year to year according to the snow and ice type and may range from 0.09—0.016 (for pure crystalline ice covered by water) to 0.96 (for fresh snow). The values of the vertical attenuation coefficients k_{snow} and k_{ice} are equal 11.6 m^{-1} for snow, 6.8—8.0 m^{-1} for white ice, 2.2—2.4 m^{-1} for crystalline ice, and 2.7—4.9 m^{-1} for mixed ice structure.

Fig. 2 [4] shows the absorption spectra of pure ice, measured by different authors in different regions. The ice absorption spectrum is similar to water spectrum from UV up to middle of IR spectral range. The ice absorption coefficient (a) is ranges from 0.1 to 0.01 m^{-1} for wavelength 300—600 nm. The maximal values of a relate to the soot and dust presence, the minimal ones to pure ice without impurities. A model developed in ref. [5] allows to compute irradiance attenuation in ice layer taking into account light absorption by pigments of the plankton and seaweed containing in ice. In this case irradiance attenuation is stronger than one given in fig. 2 (coefficient $k_{\text{ice}} \approx 0.85$ м^{-1} for wavelength 500 nm and weakly varies with wavelength).Thus in pure ice even with soot and dust presence, attenuation coefficient $k_{\text{ice}} < 0.1$ m^{-1}. For ice with plankton and seaweed $k_{\text{ice}} \approx 0.85$ m^{-1}.

Fig. 3 [4] shows the results of measurements of albedo spectra for ice and snow in different regions. Note that the ice albedo given in fig. 2 are due to snow traces on ice, bubbles, the seaweeds, dissolved substances and traces of penguins. Besides, fig. 3 data relate to the low Sun when the Fresnel reflection from the surface increases.

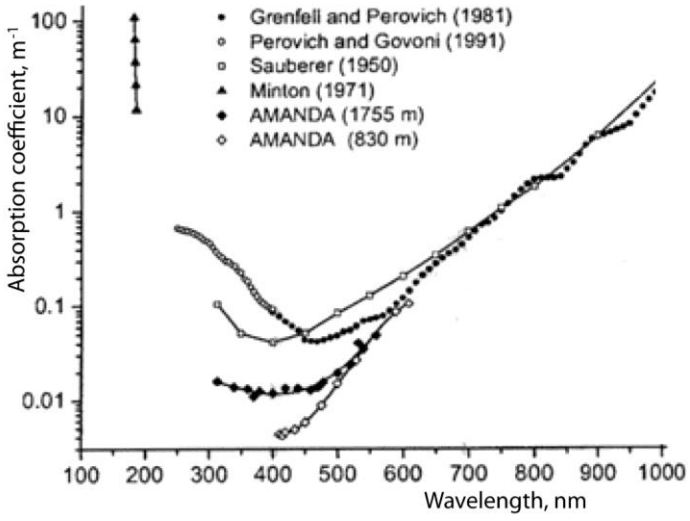

Fig. 2. Absorption spectra of pure ice [4].

Snow is mainly a scattering medium, and its scattering coefficient slightly depends on wavelength in the spectral region at 350—600 nm. Fresh snow reflects more than 90 % of the incident radiation. Based on the data of [4, 5] for 400—600 nm, the average values of vertical attenuation coefficient $k_{\text{snow}} = 12.5$ m^{-1} for fresh snow, and $k_{\text{snow}} = 7.6$ m^{-1} for old snow.

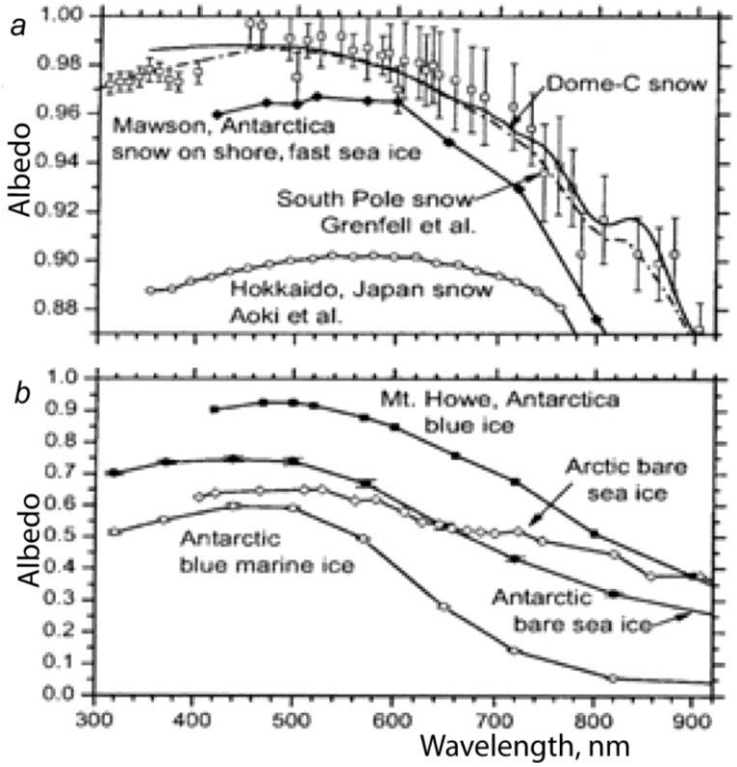

Fig. 3. Measurements of the spectral albedo of snow (*a*) and ice (*b*) surfaces [4].

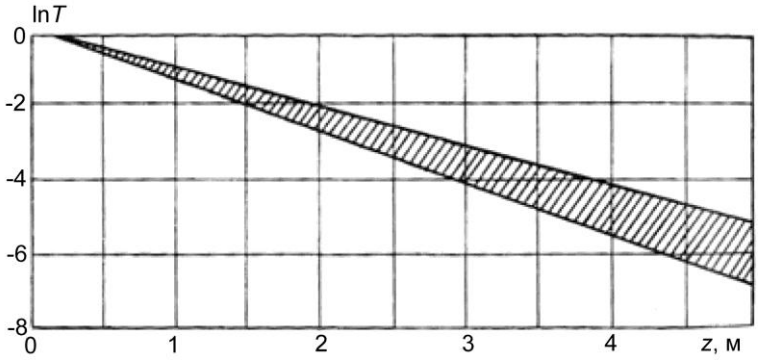

Fig. 4. Attenuation of the integral irradiance in the ice cover.
$\ln T(z) = \ln[E(z)/E(0)] = k_{ice} z$ (*z* is the ice thickness) [6].

Measurements in the Arctic give other values of albedo and light attenuation in ice [6]: albedo ranges from 4 to 12 % for young and one-year ice, and from 4 to 18 % for mature ice, while the vertical attenuation coefficient ranges from 1.1 to 1.5 m^{-1}, and its average value k_{ice} = 1.2 m^{-1} (fig. 4).

Investigations of oil properties in visual spectrum [7, 8] gave the value of real part of the refraction index n = 1.5—1.485, while the value of its complex part χ = 0.0014–0.0056. This means that albedo R of the oil film for normal incidence (we use the Fresnel equation $R = [(n-1)/(n+1)]^2$) is about 4 %, while the absorption coefficient $a = 4\pi\chi/\lambda$ for wavelength λ = 500 nm, a = (3.5—1.4) 10^4 m^{-1}, that is oil is almost opaque for radiation in visual spectral range.

Possibility of detecting the oil film on the lower surface of plane-parallel flat ice layer from above. Let us consider the case of detecting the oil film located at the lower surface of plane-parallel flat ice layer of thickness z without snow by the standard TV-system from a low (less than 1 km) altitude under natural illumination. In this case, visibility is defined by the image contrast:

$$C = (L_1 - L_2)/L_2, \tag{1}$$

where L_1 and L_2 are the apparent radiances of the polluted and not polluted ice areas expressed through radiance coefficients (remote sensed reflectance) of ice, oil and water ρ_{ice}, ρ_{oil}, ρ_{water} and ice transmittance $T = E(z)/E(0) = \exp(-k_{ice}z)$:

$$L_1 = E_0 T^2 \rho_{oil} 0.533\pi^{-1} + E_0 \pi^{-1} \rho_{ice}, \tag{2}$$

$$L_2 = E_0 T^2 \rho_{water} 0.533\pi^{-1} + E_0 \pi^{-1} \rho_{ice}, \tag{3}$$

where 0.533 is the coefficient taking into account the change of radiance due to double passing air/ice boundary.

Substituting eqs. (2), (3) in (1), we obtain:

$$C = \frac{C_0}{1 + \dfrac{\rho_{ice} \exp(2k_{ice}z)}{0.533\rho_{water}}}, \tag{4}$$

where $C_0 = (\rho_{oil} - \rho_{water})/\rho_{water}$ is the inherent contrast on the lower ice surface.

The angular distribution of radiance reflected from the oil film and ice is considered to be isotropic. Then the radiance coefficients ρ_{oil} and ρ_{ice} are equal to albedo R_{oil} and R_{ice}.

As indicated above, R_{oil} = 0.04, while R_{ice} depends on various factors and in the absence of snow, ranges from 0.02 to 0.6. The water radiance coefficient [9]:

$$\rho_w = 0.275 \frac{b_b}{a + b_b}, \tag{5}$$

where a and b_b are the absorption and backscattering coefficients.

To compute a and b_b, the small-parameter model of the seawater and the Secchi depth theory can be used [10, 11].

In the spectral range of 500 to 550 nm the absorption and backscattering coefficients can be expressed through water extinction coefficient [10]:

$$a = 0.056c + 0.048, \tag{6}$$

$$b_b = 0.018c; \tag{7}$$

$$b_b = 0.0094c + 0.00045. \tag{8}$$

Eq. (7) relates to coastal waters (Case 2 in Morel's classification), eq. (8) to ocean waters (Case 1). In accordance with Secchi depth theory, $c \approx 6/z_d$ for Case 2 waters and $c \approx 5/$ for Case 1 waters (z_d is the Secchi depth) [11].

To find the maximal ice thickness z through which the oil film at the lower ice surface can be detected, one should replace in eq.(4) C by the contrast threshold of a standard TV-system which is about 2 % and solve eq.(4) with respect to z taking into account eqs.(5)—(8). The results of such computation for ocean (z_d = 20 m) and coastal (z_d = 20 m) waters are shown in the table 1.

Table 1

Maximal ice thickness through which the oil film can be detected at the lower ice surface

Conditions	ρ_{ice}	k_{ice}, m^{-1}	z_d, m	z, m
Pure ice without impurities [4]	0.02	0.1	10	10
			20	12
Pure ice with phytoplankton pigment and algae [4, 5]	0.1	0.85	10	0.4
			20	1
Arctic, young ices [6]	0.12—0.04	1.5—1.1	10	0.1—0.7
			20	0.5—1.1
Arctic, ices of many years [6]	0.18—0.04	1.5—1.1	10	0.06—0.7
			20	0.35—1.1
Bohai Sea [12]	0.20	2.8	10	0.21
			20	0.33

Note that the image contrast will change with the water turbidity because of changing the water radiance coefficient ρ_{water}. The value of ρ_{water} decreases and the contrast C increases for purer water. In turbid water, at some value of c ($z_d \approx 6$ m), the value of ρ_{water}(550 nm) will be equal to $\rho_{oil} \approx 0.04$, and then the contrast $C = 0$. If the water turbidity further increases, the contrast becomes negative (that is, the water becomes brighter than oil). Thus, when the oil film is observed by the TV-system, it is worth to use several (not less than two) different spectral ranges: the water optical properties, in contrast to oil properties, have the distinct spectral dependence, so, if the contrast $C = 0$ in one spectral region, $C \neq 0$ in another spectral region.

Thus, if to exclude the ideal case of pure ice without impurities, which hardly can be often meet in natural conditions, observation of oil films on the lower ice surface by TV-system (in daylight the irradiance at TV-tube is always higher than the threshold irradiance) is possible for ice of thickness z less than 1 m without snow depending on ice optical parameters. Since the snow albedo is usually $\rho_{snow} > 0.9$, while $k_{snow} \approx 8$—12 m^{-1}, it is easy to check that the oil film located on the lower surface of the ice layer covered by snow cannot be detected from above, and its detection is possible only from below by an underwater imaging system using artificial illumination.

In principal, detection of pollution on the lower ice surface is possible by use of a lidar. In this case half of emitted pulse length $l = V_{ice}\Delta t$ (Δt is pulse duration, V_{ice} light velocity in the ice) must be much less than the ice thickness. For example, if $\Delta t = 1$ ns, $l = V / n_{ice} = 0.11$ m ($n_{ice} = 1.31$ is the ice refraction index, V light velocity in vacuum). Then the derivation of echo-signal with respect to time will change on the boundaries air-ice and ice-water due to different signal attenuation in air, ice and water, while the signal sharply falls on the lower ice surface covered by film because of light absorption by oil. Thus, detection of oil film by the lidar sensing may be very effective if the signal/noise ratio is sufficient.

Oil films can be detected also by the fluorescence lidar applied for determination of oil products in water [13]. We don't know about applying fluorescence lidars for detection of ice pollutions. However, detection of the oil at lower ice surface by use of pulsed UV lamp and receiver of fluorescence placed above ice, was carried out experimentally [14]. It was shown that detection of oil is possible for ice maximal thickness about 100 cm for ice from fresh water and about 80 cm for ice from seawater.

Possibility of observing the oil films on the lower surface of the ice cover by an underwater imaging system. We will consider the most advanced pulsed-laser system. The parameters of the real system produced in the Television Institute [15] are the following: the aver-

age power of the laser beam P_0 = 10W; wavelength λ = 530 nm; the diameter of the objective lens D = 20 mm; the viewing angle and the laser divergence 2β = 60°; the number of elements in the frame N = 600×600; the photo-cathode efficiency η = 0.045 A/W, frame duration t = 0.04 s. For the pulsed-laser imaging system, the distance of vision is determined by the signal / noise ratio (SNR). For a large target (in our case the oil spot) of reflectance R, SNR in the system placed at the distance Z from the target, may be calculated as [1, 2]:

$$\Psi = C\sqrt{t\eta P / e}\,,$$

$$P = \frac{P_0 D^2 R}{4NZ^2}\exp(-2a_1 Z)\,, \qquad (9)$$

where P is the signal power from the viewed target with reflectance R, placed at the distance Z from the system, $C = |(P - P_b|/P$ is the image contrast, P_b is the signal power from the background with reflectance R_b, $a_1 = a + 2b_b$ is the water effective absorption coefficient, e is the electron charge. For our case of ice and oil fields observation, ice is the target ($R = \rho_{ice}$), oil is the background ($R_b = \rho_{oil}$), and

$$P_b = PR_b / R\,. \qquad (10)$$

Computations of the SNR by eqs. (9), (10) were carried out for the same ocean (= 20 m) and coastal (z_d = 10 m) waters as above, by use of eqs. (6)—(8). Since in this case the more ρ_{ice}, the more SNR and vision distance, we chose for computation the minimal value of ρ_{ice} = 0.1 from the table 1. The results of calculation are shown in fig. 5.

One can see that the maximal vision distance of the oil film is 40 m for z_d = 20 m and about 30 m for z_d = 10 m.

Strictly speaking, the calculation given above relates to a case of observation in the nighttime. During the daytime observation visibility can worsen because of penetration into the receiver of natural light which is a source of an additional noise. However this effect can be minimized by installation of spectral filter with the transmission maximum corresponding to the wavelength of laser radiation on the receiver.

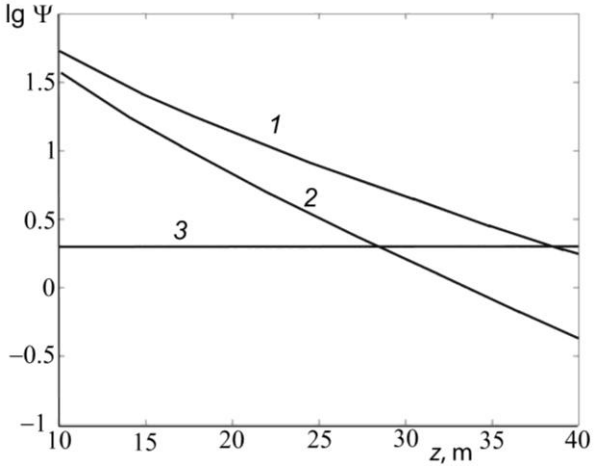

Fig. 5. Signal/noise ratio (Ψ) via distance Z of observation of the oil film on the lower ice surface by underwater laser pulsed imaging system for ocean (z_d = 20 m) (*1*) and coastal (z_d = 10 m) (*2*) waters. $\psi_{th} \cong 5$ is the SNR threshold (*3*).

Possibility of observing the oil films on the lower surface of the solid and broken ice layer from below in natural illumination. Let us consider the situation (fig. 6), when the ice surface is illuminated by diffuse light (cloudy sky), while an image is formed by the moving narrow-angle receiver. In the position 1 (fig. 6), when the receiver is directed at the not polluted ice, the apparent ice radiance:

$$L_{ice} = \pi^{-1} E_0 e^{-k_{ice} z} e^{-k_w Z}\,, \qquad (11)$$

where z is the ice thickness, Z is the depth of the receiver, $k_w = a + 2b_b$ is the vertical attenuation coefficient in water.

In the position 2, when the receiver is placed on the shadow boundary and is di-

rected to the oil spot, that is viewed point is at the distance $l_1 = Z\mathrm{tg}\,\theta$ from the oil spot edge ($\theta = \arcsin(1/n_{ice})$ is the maximal angle at which the light rays go after transmission through the ice), the radiance L_{oil} is determined by light, first scattered back (upwards) in the water layer Z and then reflected by the oil film. Then

$$L_{oil} = \pi^{-1} E_0 e^{-k_{ice} z} e^{-3k_w Z} \rho_w \rho_{oil}. \qquad (12)$$

One can see from eqs. (11) and (12) that $L_{oil} = L_{ice}\,(\rho_{oil}\rho_w \exp(-2k_w Z))$, that is apparent radiance of the oil is more than $1/(\rho_{oil}\rho_w) = 1/(0.04 \cdot 0.02) = 1000$ times greater as compared with not polluted area of ice, thus the oil-ice contrast (negative) differs little from unity. If the receiver is situated inside the shadow area at the distance $l_2 = Z_1\mathrm{tg}\,\theta$ ($Z_1 > Z$) from the oil spot boundary, the contrast will further increase. It is obvious also that under direct solar illumination or on observation through the broken ice the value of the contras will be the same.

Generally speaking, to evaluate visibility of such system, one should calculate not only the contrast, but also the irradiance at the detector photocathode. However, simple calculations show that under daylight, even when the Sun is low, this irradiance much higher than threshold one. Thus, in this case light attenuation in the ice and water obviously may be ignored.

Note also that probability of oil film detection will decrease because of variations of the contrast of ice fields due to natural variations of parameters in used equations.

Conclusion. This paper has analyzed the possibility of detecting oil films on the ice bottom from above and from below (through given water layer). The efficiency of detection depends primarily on the ice state, snow presence and observation conditions. Observation by the standard TV-system from rather low (less than 1 km) altitude is possible for the ice without snow of thickness less than 1 m only. When ice is covered by snow or includes soot, dust, aquatic plants and phytoplankton pigments, the oil films can be detected using an underwater pulsed-laser imaging system only.

Apparently the most effective way of solving the problem of detecting oil on the water-ice boundary is a combination of oil sensing from above through the ice cover and from below through water layer.

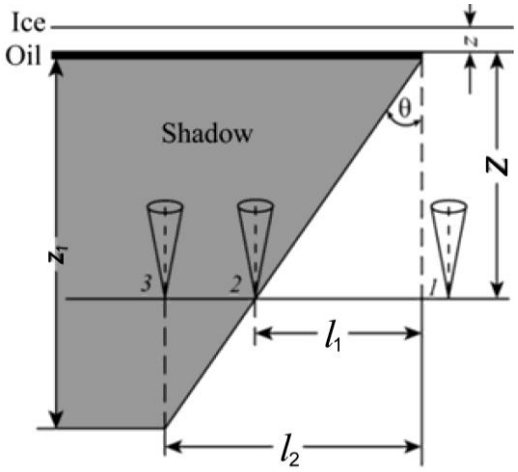

Fig. 6. Schematic diagram of the observation of oil films on the lower ice surface from below in natural illumination.

This study was supported by the Russian Foundation for Basic Research, project N 13-05-00050.

Литература

1. *Dolin L. S., Levin I. M.* Optics, Underwater // Encyclopedia of Applied Physics, Chap. 12. New York: VCH Publ., 1995. P. 571—601.
2. *Dolin L. S., Levin I. M.* Underwater Optics // The Optics Encyclopedia, 5 / Ed. by Th. G. Brown et al. Weinheim: Wiley-VCH Publ., 2004. P. 3237—3271, 2004.
3. *Petrov M., Terzhevik A., Palshin N., Zdorovennov R., Zdorovennova G.* Solar radiation regime and surface albedo of the snow-ice cover of a shallow lake // Proceedings of the III International Conference «Current Problems in Optics of Natural Waters» (ONW'2005) / Ed. by I. Levin and G. Gilbert. Proceedings of D. S. Rozhdestvensky Optical Society, St. Petersburg, Russia, 2005, p. 199—203.
4. *Warren S., Brandt R., Grenfell T.* Visible and near-ultraviolet absorption spectrum of ice from transmission of solar radiation into snow // Applied Optics. 2006. V. 45, N 21. P. 5320—5334.

5. *Jin S., Stamnes K., Weeks W.* Transport of photosynthetically active radiation in sea ice and ocean // SPIE, Ocean Optics XII (Editor J. Jaffe). 1994. V. 2258. P. 954—963.
6. *Лебедев Г. А., Сухоруков К. К.* Распространение электромагнитных и акустических волн в морском льду. СПб.: Гидрометеоиздат, 2001. 81 С.
7. *Альперович Л., Комарова А., Нарзиев Б., Пушкарев В.* Оптические постоянные нефтей в области 0.25—25 мкм // Журнал прикл. спектроскопии. 1978. № 4.
8. *Золотарев В., Китушина И., Сутовский С.* Оптические постоянные нефтей в диапазоне 0.4—15 мкм // Океанология. 1977. Т. 17, № 6. С. 1113—1117.
9. *Dolin L., Gilbert G., Levin I., Luchinin A.* Theory of Imaging Through Wavy Sea Surface. N. Novgorod: Institute of Applied Physics, 2006. 180 p.
10. *Левин И. М., Копелевич О. В.* Корреляционные соотношения между первичными гидрооптическими характеристиками в области спектра около 550 нм // Океанология. 2007. Т. 47, № 3. С. 344—348.
11. *Левин И. М., Радомысльская Т. М.* Оценка гидрооптических характеристик по глубине видимости диска Секки // Изв. РАН, Физика Атмосферы и Океана. 2012. Т. 48, № 2. С. 239—246.
12. *Xu Z., Yang Y., Wang G., Cao W., Li Z., Sun Z.* Optical properties of sea ice in Liaodong Bay, China // J. Geophys. Res., 117, C03007, doi: 10.1029/2010JC006756.
13. *Фадеев В. В., Чубаров В. В.* Количественное определение нефтепродуктов в воде методами лазерной спектроскопии // ДАН СССР. 1981. Т. 261, № 2. С. 342—346.
14. *Moir M. E., Yetman D. C.* The detection of oil under ice by pulsed ultraviolet fluorescence // Proc. 1993 International Oil Spice Conference. March 29—April 1, 1993, Tampa, Florida. (API publication No. 75-4164); P. 521—523.
15. *Алешин И. В., Гончаров В. К., Осадчий В. Ю., Левин И. М., Радомысльская Т. М., Клементьева Н. Ю., Колобков В. С., Зеленский В. В., Джун Ли.* Современные методы и технические средства обнаружения в толще морской среды аварийных утечек нефти из подводных нефтепроводов // Морской вестник. 2006. № 2 (18). С. 78—82.

Статья поступила в редакцию 11.06.2014 г.

Радомысльская Т. М., Левин И. М.
Санкт-Петербургский филиал Института океанологии им. П. П. Ширшова РАН
ocopt@yandex.ru

Возможности детектирования нефтяных загрязнений поверхности морского льда

Приводится обзор оптических свойств льда, снега и нефти, на основе которого сделаны оценки возможности детектирования нефтяных загрязнений нижней поверхности морского льда. Рассматриваются случаи наблюдения сверху с помощью стандартной телевизионной системы при дневном освещении и наблюдения снизу подводной лазерной импульсной системой и движущимся узкоугольным фотоприемником. Показано, что если исключить редкий случай чистого кристаллического льда, наблюдение сверху при естественном освещении возможно только при отсутствии снега и при толщине льда менее одного метра. Наблюдение снизу с помощью лазерной системы возможно независимо от толщины льда и присутствия снега с глубин до 30 м в прибрежных и до 40 м и более в океанских водах. Если использовать для наблюдения горизонтально перемещающийся узкоугольный приемник с осью, направленной вертикально вверх, при естественном освещении, контраст нефть–лед мало отличается от единицы.

Ключевые слова: нефтяные загрязнения, морская поверхность, лед, снег, морская вода, подводное видение.